ELSEVIER

Journal of Nuclear Materials 241–243 (1997) 283–287

journal of nuclear materials

Plasma–neutral gas interaction in a tokamak divertor: Effects of hydrogen molecules and plasma recombination

S.I. Krasheninnikov [a,d,*], A.Yu. Pigarov [b,d], T.K. Soboleva [c,d], D.J. Sigmar [a]

[a] *Massachusetts Institute of Technology, Plasma Fusion Center, 167 Albany Street, Cambridge, MA 02139, USA*
[b] *Princeton University, Plasma Physics Laboratory, James Forrestal Campus, P.O. Box 451, Princeton, NJ 08543, USA*
[c] *Instituto de Ciencias Nucleares, Universidad Nacional Autonoma de Mexico, Apdo. Postal 70-543, 04510 Mexico D.F., Mexico*
[d] *I.V. Kurchatov Institute of Atomic Energy, 1 Kurchatov Sq., Moscow 123098, Russia*

Abstract

We investigate the influence of hydrogen molecules on plasma recombination using a collisional-radiative model for multispecies hydrogen plasmas and tokamak detached divertor parameters. The rate constant found for molecular activated recombination of a plasma can be as high as 2×10^{-10} cm^3/s, confirming our pervious estimates. We investigate the effects of hydrogen molecules and plasma recombination on self-consistent plasma–neutral gas interactions in the recycling region of a tokamak divertor. We treat the plasma flow in a fluid approximation retaining the effects of plasma recombination and employing a Knudsen neutral transport model for a 'gas box' divertor geometry. For the model of plasma–neutral interactions we employ we find: (a) molecular activated recombination is a dominant channel of divertor plasma recombination; and (b) plasma recombination is a key element leading to a decrease in the plasma flux onto the target and substantial plasma pressure drop which are the main features of detached divertor regimes.

Keywords: ALCATOR C-MoD; Divertor plasma; 1D model; Detached plasma; Particle balance

1. Introduction

Recent experiments on most diverted tokamaks have demonstrated the so-called detached divertor regimes [1–4]. These regimes are characterized by a low plasma temperature near the divertor plates (of the order of 1 eV), and a strong decrease of the plasma particle flux onto the plates. Plasma recombination [5–7] in the divertor region seems the most probable explanation of the decrease of the plasma particle flux in detached divertor regimes. Ref. [8] found that apart from conventional three-body plasma recombination, the molecular activated recombination (MAR) involving vibrationally excited molecular hydrogen, $H_2(v)$, (through the ion conversion reaction $H_2(v) + H^+ \rightarrow H_2^+ + H$ followed by dissociative recombination $H_2^+ + e \rightarrow 2H$) can be a very important mechanism of extinguishing plasma in a tokamak divertor. Moreover, the estimates of the MAR rate constant, $K_{MAR} \sim 3 \times 10^{-10}$ cm^3/s, obtained in Ref. [8], led to the conclusion that for C-Mod conditions the local plasma particle sink due to the MAR process, $n_e[H_2]K_{MAR}$ (n_e and $[H_2]$ are the electron and molecular hydrogen densities), can even exceed plasma particle sink from conventional radiative and three-body recombinations.

In this paper we will present: (a) the dependencies of K_{MAR} on the plasma and neutral gas parameters by applying a collisional-radiative (CR) model for detached divertor plasma conditions, and (b) the results of a self-consistent modeling of the plasma flow in the recycling region for a 'gas box' neutral transport model [9] taking into account both three-body and molecular activated recombinations.

* Corresponding author. Tel.: 617 253 0478; fax: 617 253 0448; e-mail: krash@rex.pfc.mit.edu.

PII S0022-3115(96)00515-6

2. Collisional-radiative model for multispecies hydrogen divertor plasmas

The CR theory originally developed by Bates [10], has been applied to various atomic and molecular electronic structures [10–13]. The kinetics of vibrational level excitation and chemical reactions for molecules can also be studied within a framework of the CR model [14]. Our CR model involves the ground, vibrationally and electronically excited states of hydrogen molecules H_2 and molecular ions H_2^+, the ground H_0 and excited H^* states of hydrogen atoms, and positive H^+ and negative H^- hydrogen ions. The model incorporates an extensive atomic–molecular data set including the chemical reactions which have been found to be important for the tokamak divertor plasmas [8,15], and various laboratory and astrophysical plasmas [16–23].

We consider plasma conditions typical for detached divertor plasma: electron temperature ranges of $1 < T_e < 5$ eV; a hot plasma ion component as well as atomic–molecular mixture of the neutral gas with the temperatures about T_e; plasma densities n_e varying from $\sim 10^{13}$ cm^{-3} to $\sim 10^{15}$ cm^{-3}; and gas densities $[H_2]$, $[H] \le n_e$. Since the lifetime of H_2^+, H^-, and H^* with respect to CR decay is very short ($< 10^{-7}$ s), the relative concentration of these particles is small compared to the electron and neutral gas densities. Therefore we neglect: (a) all collision processes in which both collision partners are in the excited states; (b) the contribution of reactions which take place in collisions between H_2^+, H^-, and H^*; (c) electron impact excitation of electronic states of H_2 with respect to the molecule dissociation via excitation of the lowest repulsive triplet state $b^3\Sigma_u^+$. We exclude from the description: (a) formation of very heavy particles such as H_m^+, $m > 2$; (b) processes of electron attachment to atoms; and (c) various associative reactions proceed via triple collisions of heavy particles. Then, our kinetic scheme for divertor plasma recombination is based on the following set of reactions:

$$
\begin{aligned}
&H_2(v) + e \rightarrow H_2(v') + e\\
&H(n) + H^+ \rightarrow 2H^+ + e\\
&H_2(v) + H^+ \rightarrow H_2(v') + H^+\\
&H(n) \rightarrow H(n') + \hbar\nu, \quad n > n'\\
&H_2(v) + H \rightarrow H_2(v') + H\\
&H_2^+(v) + H \rightarrow H_2^+(v') + H\\
&H_2(v) + H_2(v') \rightarrow H_2(w) + H_2(w')\\
&H_2^+(v) + H^+ \rightarrow H_2^+(v') + H^+\\
&H_2(v) + e \rightarrow H + H^-\\
&H_2^+(v) + e \rightarrow H + H(n), \quad n > 1\\
&H_2(v) + e \rightarrow 2H + e\\
&H_2^+(v) + e \rightarrow H^+ + H(n) + e\\
&H_2(v) + H^+ \rightarrow H_2^+(v') + H\\
&H^- + H^+ \rightarrow H + H(n)\\
&H_2(v) + e \rightarrow H_2^+(v') + 2e\\
&H^- + e \rightarrow 2e + H(n)\\
&H_2(v) + e \rightarrow H + H^+ + 2e\\
&H^- + H \rightarrow 2H + e\\
&H(n) + e \rightarrow H(n') + e\\
&H^+ + 2e \rightarrow H(n) + e\\
&H(n) + H^+ \rightarrow H(n') + H^+\\
&H^+ + e \rightarrow H(n) + \hbar\nu\\
&H(n) + e \rightarrow H^+ + 2e
\end{aligned}
\qquad (1)
$$

where v and n are the vibrational and principal quantum numbers, respectively.

In reaction set (1) there are three reaction chains which lead to recombination in a tokamak divertor plasma: (a) conventional ion–electron recombination (e/i) which include radiative and three-body recombination processes, and MAR which includes (b) atomic to molecular ion conversion with a consequent dissociative recombination of the molecular ion [8], and (c) dissociative attachment of an electron to molecular hydrogen with a consequent reaction of mutual neutralization of the negative ion and proton [15]. Thus, the plasma continuity equation can be written in the form

$$\partial n_e/\partial t + \nabla\vec{j} = K_{ion} n_e N - K_{(e/i)} n_e^2 - K_{MAR} n_e [H_2], \quad (2)$$

where N and K_{ion} are the density and effective ionization rate constant of the neutral gas; $\vec{j}$ is the plasma flux; $K_{(e/i)}$ and K_{MAR} are the radiative and three-body, and molecular activated recombination rate constants, respectively.

We solve the set of kinetic equations for Eq. (1) in a quasi-stationary and quasi-homogeneous approximation by using the CRAMD code [24]. We assume that the temperatures of the electrons, ions, and atomic hydrogen are equal, T, while the temperature of molecular hydrogen is $0.5T$. We choose the following relation between the neutral and plasma densities $[H_2] = [H] = 0.1 n_e$ (notice that the dependence of K_{MAR} on the ratio n_e/N is rather weak) and assume that the plasma is transparent to radiation. The dependencies of molecular hydrogen ionization rate constant, $K_{ion}^{H_2}$, $K_{(e/i)}$ and K_{MAR} on the temperature T, found by solving kinetic Eq. (1), are shown in Fig. 1 for two plasma densities (10^{14} and 10^{15} cm^{-3}). One sees that the maximum of K_{MAR} reaches 2×10^{-10} cm^3/s, in good agreement with our earlier estimates [8]. The decrease of K_{MAR} with increasing plasma density is caused by the increasing ionization of excited atoms H^* which form during the dissociative recombination of molecular ions. From Fig. 1 we can find that the plasma sink due to the

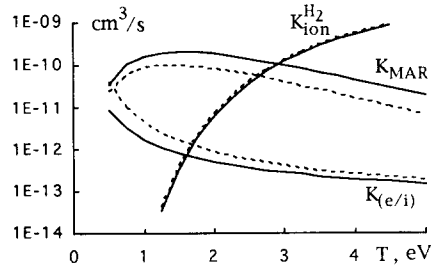

Fig. 1. The dependencies of $K_{ion}^{H_2}$, $K_{(e/i)}$, and K_{MAR} on the temperature T, found from the solutions of kinetic Eq. (1), for two plasma densities 10^{14} cm^{-3} (solid) and 10^{15} (dashed) cm^{-3}.

MAR exceeds the ionization source for temperatures $T \leq 3$ eV.

3. Plasma flow in the recycling region and recombination effects

3.1. Geometry

We consider the Knudsen regime of neutral gas flow in a divertor (neutral mean free path λ_N larger than the plasma width Δ_p). We assume (see Fig. 2) that at a poloidal distance L_N from the plate there is the widening of the divertor slot (which we will call a 'gas box') to the width, Δ_{gb}, which is much bigger than the slot width Δ far from the target. For the case when the ratio δ_{gb}/L_N is not too small and $\Delta/L_N \ll 1$ we can assume a uniform distribution of neutral gas within the 'gas box' and neglect plasma–neutral interaction outside the 'gas box' [9]. Moreover, since $\lambda_N > \Delta_p$ and recombination of hydrogen atoms of the sidewalls is rather strong, we assume that the neutral component consist of the molecular species.

3.2. Equations

We prescribe the plasma pressure, P_u, and incoming energy flux, q_{rc}, at the entrance into the 'gas box'. Using y as the 'poloidal' coordinate directed from the target, plasma parallel momentum (in subsonic approximation) as well as plasma energy (describing both ion–neutral elastic and electron–neutral inelastic collisions) balance equations and continuity equation can be written in the form

$$j = -\left(b^2/MNK_{iN}\right)(\mathrm{d}P/\mathrm{d}y), \tag{3}$$

$$\mathrm{d}q/\mathrm{d}y = -\varepsilon n_e N K_{iN} - E_{ion} n_e N K_{ion}^{H_2} - T n_e\left(f_{(e/i)} K_{(e/i)} n_e + f_{MAR} K_{MAR} N\right), \tag{4}$$

$$\mathrm{d}j/\mathrm{d}y = K_{ion}^{H_2} n_e N - K_{(e/i)} n_e^2 - K_{MAR} n_e N, \tag{5}$$

where $P = 2n_eT$ is the plasma pressure; N is the neutral gas density; M is the ion mass; $b = \sin\psi$ with ψ the angle between the target and magnetic field line; $j = bnV$ is the poloidal plasma flux with V the parallel plasma velocity; E_{ion} is the ionization 'cost' describing plasma energy losses due to electron–neutral inelastic collisions per ionization event; $K_{iN} = 2.1\sigma_{iN}(T/M)^{1/2}$ with σ_{iN} the ion–neutral collision cross section, which is assumed to be constant; $\varepsilon(T) = (T - T_0)\bar{\varepsilon}$ is the characteristic energy loss due to elastic ion–neutral collisions with $\bar{\varepsilon} = 1.5$ and T_0 the neutral gas temperature; $f_{(e/i)}$ and f_{MAR} describe plasma kinetic energy loss due to (e/i) and molecular activated recombinations; $q = 5Tj + q_e$; and $q_e = -\kappa_e(T)b^2\,\mathrm{d}T/\mathrm{d}y$ are the total and conductive poloidal plasma energy fluxes with $\kappa_e(T)$ the parallel electron heat conduction coefficient.

3.3. Boundary conditions

The boundary conditions for Eqs. (3)–(5) are

$$q(y = L_N) = -q_{rc}, \qquad j(y = L_N) = 0,$$
$$P(y = L_N) = P_u, \qquad q(y = 0) = \delta j(y = 0)T_d,$$
$$j(y = 0) = -(\alpha b P_d C_d/2T_d), \tag{6}$$

where $(\ldots)_d$ denotes value of $(\ldots)$ near the target ($y = 0$), $C_d = (T_d/M)^{1/2}$, $\alpha \approx 0.5$, and δ is the plasma heat transmission coefficient. Recall that P_u and q_{rc} are the pre-

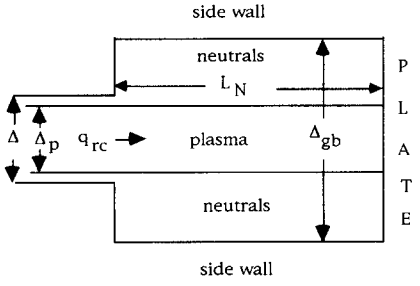

Fig. 2. Geometry of the problem.

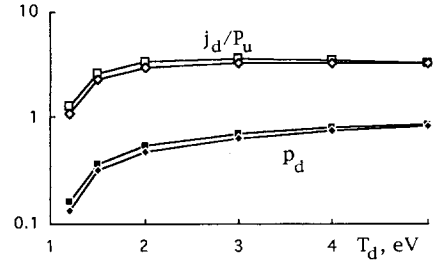

Fig. 3. Normalized plasma flux onto the target, j_d/P_u (10^3 cm/s eV) and plasma pressure drop, $p_d = P_d/P_u$, as the functions of plasma temperature at the target T_d, with recombination for $L_N = 5$ cm, and $P_u = P_0 \equiv 10^{16}$ cm^{-3} eV (squares) and $0.25P_0$ (diamonds).

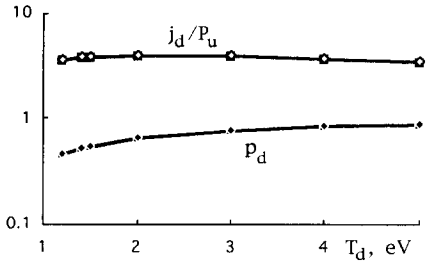

Fig. 4. The same as in Fig. 3, but without recombination.

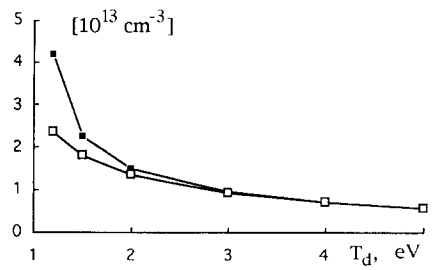

Fig. 6. The neutral gas density as a function of plasma temperature at the target T_d, for $L_N = 5$ cm with and without (open squares) recombination.

scribed upstream plasma pressure and heat flux coming into the 'gas box' region from upstream. Notice that there are 5 boundary conditions for two second order differential Eqs. (4) and (5) for plasma pressure and temperature. Therefore, they can only be satisfied for some specific neutral density N, which has to be found by solving Eqs. (3)–(5) with the boundary conditions (Eq. (6)).

3.4. Results of numerical solutions

Eqs. (3)–(6) are solved numerically. We use the rate constants $K_{ion}^{H_2}$, and K_{MAR} found from our CR model and take the following input parameters $\alpha = 0.5$, $\delta = 5$, $b = 0.05$, $f_{(e/i)} = 1.5$, $f_{MAR} = 3$, and $T_0 = 1$ eV. We use the shooting method to numerically solve Eqs. (3)–(6) by fixing the plasma temperature near the target T_d and adjusting the plasma pressure near the target and the neutral gas density N to the boundary conditions at the target and at the entrance into the 'gas box'. We solve Eqs. (3)–(6) for the upstream plasma pressure $P_u = P_0 \equiv 10^{16}$ cm^{-3} eV and $P_u = 0.25P_0$ and for the length $L_N = 5$ and 100 cm.

In Fig. 3 the normalized plasma flux onto the target, j_d/P_u, and the plasma pressure drop, $p_d = P_d/P_u$, are shown as functions of plasma temperature at the target T_d for $L_N = 5$ cm and $P_u = P_0$, and $P_u = 0.25P_0$. The same dependencies are shown in Fig. 4, but with both MAR and electron–ion recombination turned off. We see that without recombination and in agreement with the results of Ref. [9] there is practically no decrease in j_d/P_u and the pressure drop p_d is rather modest (unless T_d approaches very close to T_0 [9]), while with recombination turned on there is a strong decrease of both j_d/P_u and p_d at temperatures below 2 eV. There are two reasons for this behavior. First, at low plasma temperatures the plasma recombination sinks due to MAR, $S_{MAR} = \int_d y K_{MAR} n[H_2]$ (which is dominant at low T_d), and radiative and three-body recombinations, $S_{(e/i)} = \int_d y K_{(e/i)} n^2$, become comparable to the plasma ionization source, $S_{ion} = \int_d y K_{ion}^{H_2} nN$, resulting in the decrease in j_d/P_u (see Fig. 5). Second, the neutral gas density N increases with recombination turned on (see Fig. 6) to balance the steeper plasma density profile (caused by recombination!) in the expression for the plasma flux (Eq. (3)); simultaneously increasing N results in a decrease in the plasma flux onto the target which is roughly proportional to P_u/NL_N.

In Ref. [9] was shown that without plasma recombination the magnitude of L_N has a rather little effect on the dependencies of j_d/P_u and p_d on T_d. In Fig. 7 the dependencies of j_d/P_u and p_d on T_d with recombination turned on and for $L_N = 100$ cm are shown. Comparing Fig. 3 and Fig. 7 one finds that although a strong variation of L_N alter the numbers, the overall picture remains qualitatively the same.

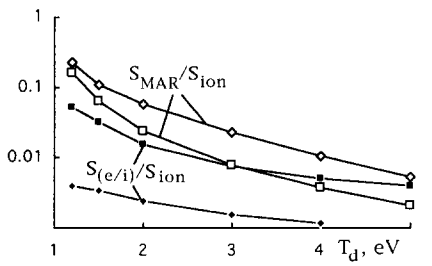

Fig. 5. Ratios of plasma recombination sinks due to MAR, S_{MAR}, and radiative and three body recombination, $S_{(e/i)}$, to the plasma ionization source, S_{ion}, as the functions of plasma temperature at the target T_d, for $L_N = 5$ cm, and $P_u = P_0 \equiv 10^{16}$ cm^{-3} eV (squares) and $0.25P_0$ (diamonds).

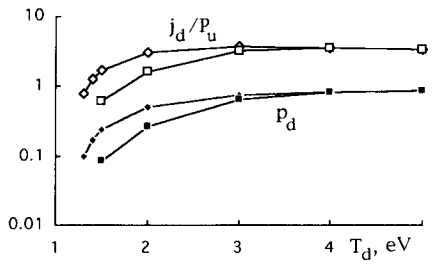

Fig. 7. The same as in Fig. 3 but for $L_N = 100$ cm.

4. Conclusions

(i) We have calculated the influence of hydrogen molecules on plasma recombination using a collisional-radiative model for multispecies hydrogen plasmas. We find that the rate constant of molecular activated plasma recombination (which mainly goes through the ion conversion reaction $H_2(v) + H^+ \rightarrow H_2^+ + H$ followed by an almost instantaneous dissociative recombination $H_2^+ + e \rightarrow 2H$) can be as high as 2×10^{-10} cm^3/s, confirming our previous estimates [8].

(ii) For the model of plasma–neutral interaction we employ the MAR is a dominant channel of divertor plasma recombination at low plasma temperature $T_d \geq T_0$.

(iii) Plasma recombination is a key element leading to divertor plasma detachment (decrease of the plasma flux onto the target and a plasma pressure drop) in our model of plasma–neutral interactions in the recycling region. Notice that the same conclusion was arrived at in Refs. [6,7] where more sophisticated neutral transport models (but without MAR) were adopted.

(iv) To make more quantitative conclusions about the impact of molecular effects on divertor plasma recombination in current experiments and ITER a more sophisticated modeling of plasma and multispecies gas transport in the divertor is required.

Acknowledgements

Work performed under DOE grants DE-FG02-91-ER-54109 at MIT, DE-AC02-76-CHO-3073 at PPPL, and under project ES104393 DGAPA-UNAM. S.I.K. is pleased to acknowledge the hospitality and support of the Instituto de Ciencias Nucleares, UNAM at Mexico City during the final stages of this work. A.Yu.P. gratefully acknowledges the hospitality and support of the PPPL.

References

[1] I.H. Hutchinson et al., Phys. Plasmas 1 (1994) 1511.
[2] G. Janeschitz et al., Proc. of 19th European Conf. on Controlled Fusion and Plasma Physics, Insbruck, 1992, Vol. 16C, Part II, p. 727.
[3] T.W. Petrie et al., J. Nucl. Mater. 196–198 (1992) 848.
[4] V. Mertens et al., Proc. of 20th European Conf. on Controlled Fusion and Plasma Physics, Lisboa, 1993, Vol. 17C, Part I, p. 267.
[5] S.I. Krasheninnikov and A.Yu. Pigarov, 11th IAEA Conf. on Plasma Phys. and Controlled Nuclear Fusion Research, Kyoto, 1986, Vol. 3, p. 387.
[6] D.A. Knoll, P.R. McHugh, S.I. Krasheninnikov and D.J. Sigmar, Phys. Plasmas 3 (1996) 293.
[7] F. Wising, D.A. Knoll, S.I. Krasheninnikov, T.D. Rognlien and D.J. Sigmar, Contrib. Plasma Phys. 36(2–3) (1996).
[8] S.I. Krasheninnikov, A.Yu. Pigarov and D.J. Sigmar, Phys. Lett. A 214 (1996) 285.
[9] S.I. Krasheninnikov and T.K. Soboleva, Phys. Plasmas 3 (1996) 2280.
[10] D.R. Bates, A.E. Kingston and R.W.P. McWhirter, Proc. R. Soc. A 267 (1962) 297; A 270 (1962) 155.
[11] H.W. Drawin and F. Emard, Z. Physik 243 (1971) 326; Physica 85C (1977) 333.
[12] J. Spence and H.P. Summers, J. Phys. B 19 (1986) 3749.
[13] K. Sawada and T. Fujimoto, J. Appl. Phys. 78 (1995) 2913.
[14] M. Capitelli, C. Gorse and A. Richard, in: Non-Equilibrium Vibrational Kinetics, ed. M. Capitelli, Ser. Topics in Current Physics, Vol. 39 (Springer-Verlag, Berlin, 1986).
[15] D.E. Post, J. Nucl. Mater. 220–222 (1995) 143.
[16] F. Linder, R.K. Janev and J. Botero, in: Atomic and Molecular Processes in Fusion Edge plasmas, ed. R.K. Janev (Plenum Press, New York, 1995) p. 397.
[17] D.K. Otorbaev, M.C.M. van de Sanden and D.C. Schram, Plasma Sources 4 (1995) 293.
[18] P. Berlemont, D.A. Skinner and M. Bacal, Rev. Sci. Instrum. 64 (1993) 2721.
[19] M.J. de Graaf et al., Phys. Rev. E 48 (1993) 2098.
[20] M.B. McElroy, Space Sci. Rev. 14 (1973) 460.
[21] T. Majeed and J. McConell, Planet Space Sci. 39 (1991) 1715.
[22] D.E. Artems and J.M. Wadehra, Phys. Rev. A 42 (1990) 5201.
[23] Z.H. Top and M. Baer, Chem. Phys. 25 (1977) 1.
[24] A.Yu. Pigarov, D.P. Stotler and C.F.F. Karney, Bull. Am. Phys. Soc. 40 (1995) 1884.